

EXTREMAL ANALYSIS OF FLOODING RISK AND MANAGEMENT

CHENGXIU LING, JIAYI LI, YIXUAN LIU, AND ZHIYAN CAI

ABSTRACT. Catastrophic losses caused by natural disasters receive a growing concern about the severe rise in magnitude and frequency. The constructions of insurance and financial management scheme become increasingly necessary to diversify the disaster risks. Given the frequency and severity of floods in China, this paper investigates the extreme analysis of flood-related huge losses and extreme precipitations using Peaks-Over-Threshold method and Point Process (PP) model. These findings are further utilized for both designs of flood zoning insurance and flooding catastrophic bond: (1) Using the extrapolation approach in Extreme Value Theory (EVT), the estimated Value-at-Risk (VaR) and conditional VaR (CVaR) are given to determine the cross-regional insurance premium together with the Grey Relational Analysis (GRA) and the Technique for Order Preference by Similarity to an Ideal Solution (TOPSIS). The flood risk vulnerability and threat are analyzed with both the geography and economic factors into considerations, leading to the three layered premium levels of the 19 flood-prone provinces. (2) To hedge the risk for insurers and reinsurers to the financial market, we design a flooding catastrophe bond with considerate trigger choices and the pricing mechanism to balance the benefits of both reinsurers and investors. To reflect both the market price of catastrophe risk and the low-correlated financial interest risk, we utilize the pricing mechanism of Tang and Yuan (2021) to analyze the pricing sensitivity against the tail risk of the floods' disaster and the distortion magnitude and the market risk through the distortion magnitude involved in Wang's transform. Additionally, our trigger process is carefully designed using a compound Poisson process modelling both the frequency and the layered intensity of the flood disasters. Finally, constructive suggestions and policies are proposed concerning the flood risk warning and prevention.

Keywords: Extreme value theory, Peaks-Over-Threshold, CAT bond Pricing, Grey Relational Analysis, Multiple-Criteria Decision-Making, Point Process, Vasicek Model, Distortion Measure

arXiv:2112.00562v1 [q-fin.RM] 1 Dec 2021

1. INTRODUCTION

Extreme weather events pose great threats to human lives and cause significant financial losses. Climate changes in recent decades increase the occurrence and the severity of such events ([1]). Extreme precipitations, as one of the extreme weather events, usually come along with management threats such as severe floods. In Asian monsoon season, the precipitations usually will trigger floods, especially in the basin of the largest river in China ([9], [14]). The historic large floods in China in the past three decades have caused over 200 billion dollars per decade ([9]). In August, 2021, the devastating floods in the Chinese city of Zhengzhou saw 457.5 millimeters of precipitation within 24 hours, which caused severe flooding and a resulting-in RMB 53.2 billion economic losses and more than RMB 6.4 billion in insurance claims resulted from over 4×10^5 cars damages. Such extreme severe disaster occurs so frequently all over the world. Despite hazard mitigation efforts and scientific and technological advances, extreme weather events continue to cause substantial losses. The concern of this paper is to develop quantitatively an insurance and financial risk management scheme to diversify the high layers of flood risks.

Extreme Value Theory (EVT) is a useful tool to evaluate and simulate extreme data of such kind of weather events, as well as financial crises, super-spreading of contagious diseases e.g., COVID-19, severe rainstorms etc ([2], [4], [5], [15]). The mis-specifications of tail risks might result in underestimating potential risks, causing the mighty breakdowns of health care systems involved. There are generally two methods to analyze extremes. One is the Block Maxima (BM) approach, which extracts maximum values of each block from the time series. Another approach is the Peaks-Over-Threshold (POT) approach, which analyzes threshold-excess by generalized Pareto (GP) models. By Fisher-Tippett theorem, the Block Maxima data is usually fitted with Generalized Extreme Value (GEV) distribution. Both methods have a common challenge to overcome the distribution uncertainty when identifying extremes as well as the rareness of extreme data, see [5, 6].

In this paper, we focus on the risk management of flooding risk in China based on the economic loss and precipitations in 2006-2018 following the workflow in Figure 1 below. First, it turns out that both possess extreme features fitted well by extreme value models, see Section 3.1. Given the various climate and topography imposed to the flood-prone regions in China together with different economic development, we implement Multiple-Criteria Decision-Making methods ([7, 8, 12, 17]) to design the layered and cross-regional insurance compensation scheme to diversify the extreme flooding risk in the framework of extreme statistics and risk management in Section 3.2. Additionally, concerned with the financial loss caused by super severe flood disasters, we consider the risk mitigation from the reinsurance to financial markets by designing catastrophe (CAT) bond as a financial instrument of re-insurance in Section 3.3, so that financial resilience can be increased ([1, 13, 18]). Indeed, the Chinese financial market is ready to issue the CAT bond in the Hong Kong market through special-purpose insurance companies to transfer catastrophe risk loss, according to the China Banking and

Insurance Regulatory Commission. The issuer can exempt or delay the payment of part of the bond principal and interest or even all of them when actual catastrophe loss exceeds the agreed amount.

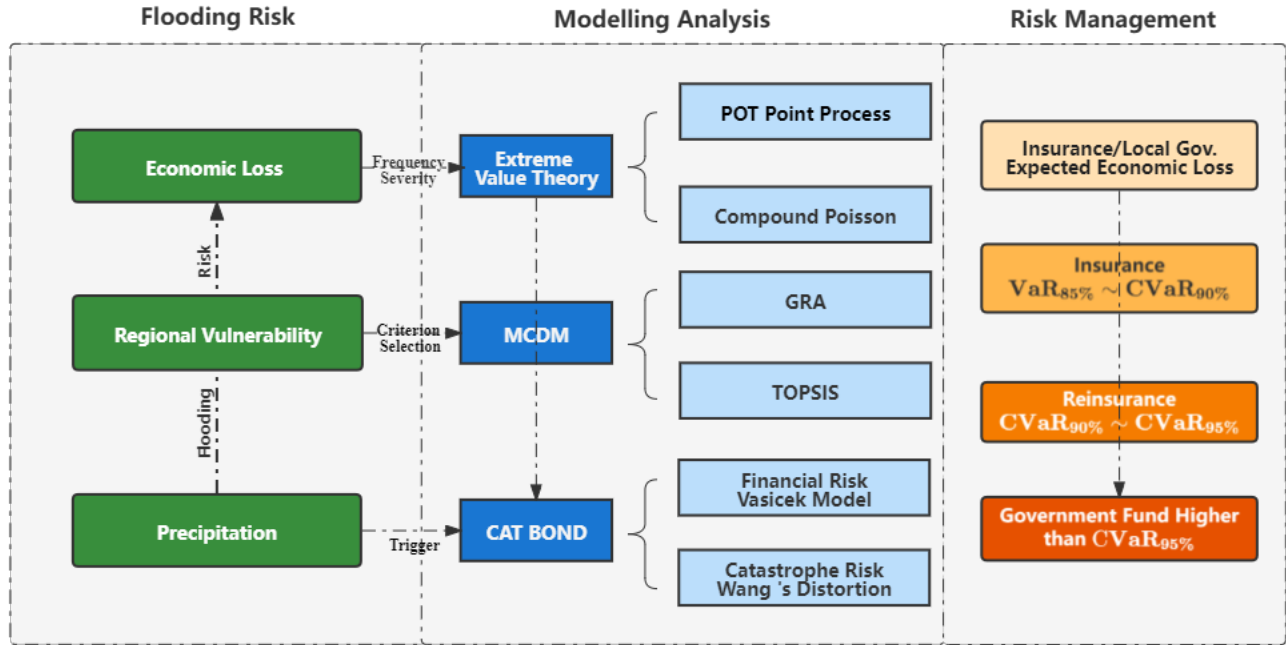


FIGURE 1. Workflow of flooding risk management.

The main contributions of the paper are three-fold.

- The layered compensation insurance scheme is well designed according to the estimated Value-at-Risk (VaR) and conditional VaR (CVaR), incorporating the extrapolation method in extreme value theory, see Table 4. This provides policy-makers constructive suggestions for allocating abundant monetary support and flood risk prevention among all stakeholders.
- In the design of cross-regional insurance fund, the sensitivity of criterion selection and weight is studied in terms of Multiple-Criteria Decision-Marking (MCDM) method using the Grey Relational Analysis (GRA) and the Technique for Order Preference by Similarity to an Ideal Solution (TOPSIS). It can ensure the mitigation of catastrophe risk within these areas to a greater extent, see Tables 6 and 7.
- The pricing mechanism of a flooding catastrophe bond is studied with considerate trigger choice concerning both the frequency and the layered intensity of the flood disasters via the maximum precipitation. Given the climate changes and financial volatility, the pricing sensitivity of both precipitation severity and financial market distortion convinces the investors and reinsurers of the pricing trend, see Figure 9.

The paper is organized as follows. Section 2 shows the regional and extreme features of max point precipitation and the caused flooding economic losses. Section 3 is devoted to the main results

followed by Section 4 for the conclusions. We end this paper with an appendix in Section 5, including all technique and methodology involved.

2. DESCRIPTIVE ANALYSIS OF FLOODING CATASTROPHE LOSS AND EXTREME PRECIPITATIONS

In order to study the catastrophe losses caused by flooding in various regions in China, economic losses of main flooding events as well as its maximum point precipitations (the maximum accumulated precipitation in a particular site within exactly 24 hour) in 31 provinces of China from 2006 to 2018, which are collected from <http://www.mwr.gov.cn/sj/>, the official website of the Ministry of Water Resources of the People’s Republic of China. Given the money inflation, all economic loss data is normalized according to 2019 annual consumer price index (CPI).

We see from Table 1 that, the average economic loss of the main flooding events in China from 2006 to 2018 is RMB 15.45 billion with a large range from RMB 0.12 billion to RMB 78.65 billion. The economic loss is roughly right-skewed with large kurtosis 5.56, confirmed also by the histogram in Figure 2. Moreover, the max point precipitation behaves similarly with certain right skewness and deviates slightly from normal distribution as well. Indeed, the precipitation, one of the most main drivers of floods, is free of human manipulation. Figure 2 shows positive association between economic loss on log scale and max-point precipitations with correlation 0.45. This motivates our trigger design of precipitation level for the catastrophe bond in Section 3.3. In particular, the 70%, 80%, 90% and 95% quantile precipitations are 626, 744, 849 and 985, respectively.

TABLE 1. Descriptive analysis of economic loss and maximum point precipitation.

Variable	Size	Min	Median	Mean	Max	Skewness	Kurtosis
Economic loss (billion RMB)	94	0.12	9.69	15.45	78.65	1.72	5.56
Max Point precipitation (mm)	94	75	479.5	530.07	1426	0.79	3.65

source: <http://www.mwr.gov.cn/sj/>, the Ministry of Water Resources of China.

In order to find the hot-spot regions of flooding risks and propose corresponding regional tackles, we summary the average economic loss of each province in 2006~2019. It shows a big spatial discrepancy from province to province. We see in Figure 3 that, the average loss ranges from RMB 2.49 billion of Shanghai to RMB 225.25 billion of Guangdong with average of RMB 74.29 billion. The regional difference of flooding risks is roughly reflected by the economic total loss. On the other hand, each province was exposed to timely-varying flooding risk with standard deviation of yearly provincial loss ranging from 3.04 of Ningxia to 204.85 for Hubei. Actually, a variety of disaster-inducing factors, risk tolerance and economic development level can systemically affect the flooding-caused loss among different regions. Therefore, the flooding related risk vulnerability level in different zones should be comprehensively considered.

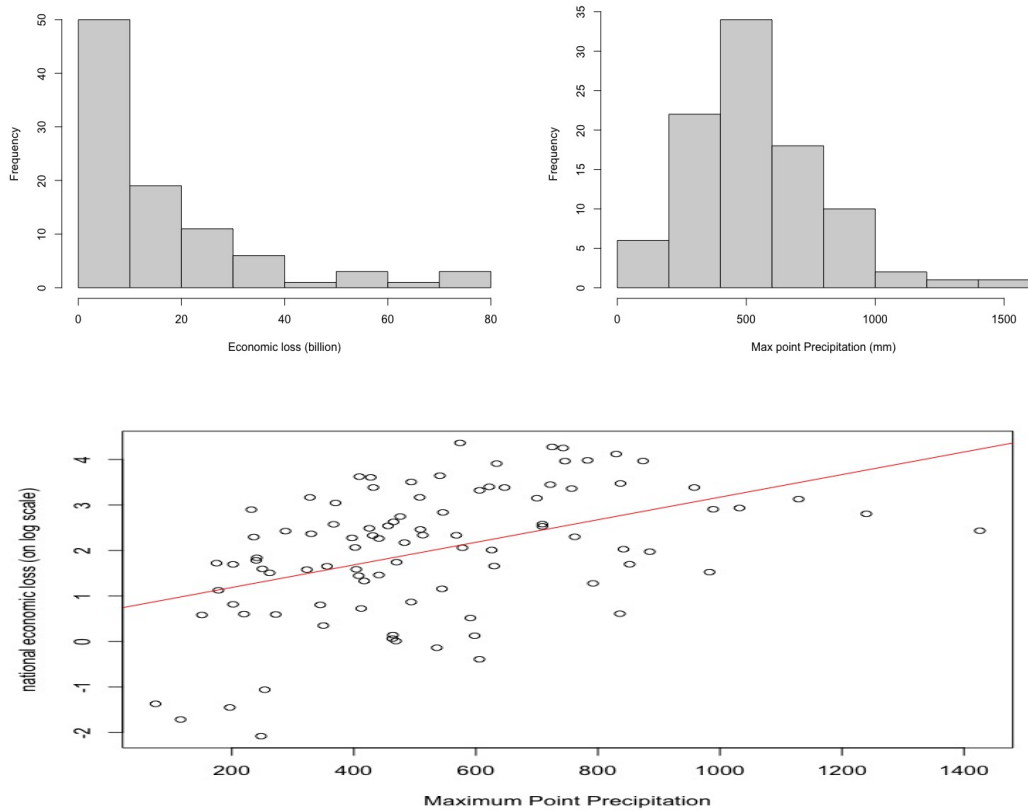


FIGURE 2. Histogram of economic loss (top left) and maximum point precipitation (top right) and scatter plot of economic loss against max point precipitation (bottom).

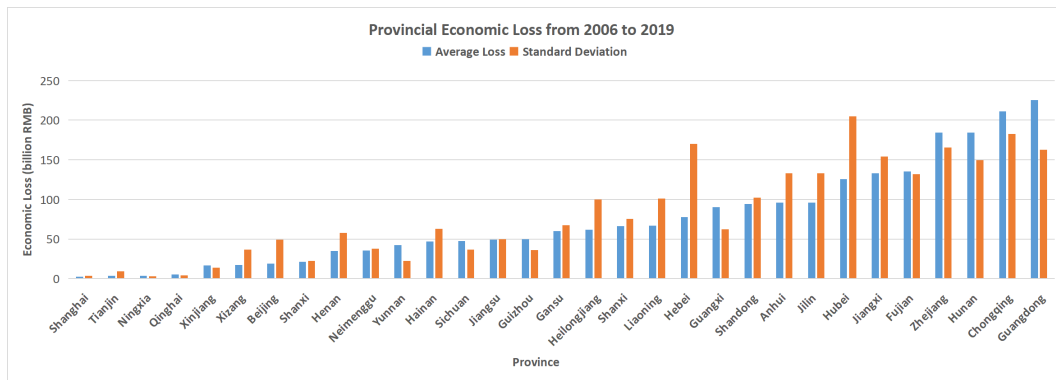


FIGURE 3. Provincial average economic loss in blue and standard deviation in orange from 2006 to 2019. Data is from <http://www.mwr.gov.cn/sj/tjgb/zgshzhgb/>, the Ministry of Water Resources of China.

This motivates our study on cross-regional insurance fund using multiple-criterion decision-making method in Section 3.2. For simplicity, we focus on the flooding vulnerability in 2019 and consider 19 provinces as representatives of different economic loss levels in Figure 3, which are located in the

TABLE 2. Flood catastrophe vulnerability evaluation indicators

Group	Label	Description	Units
Risk Exposure	X_1	Suffered Population	10000 persons
	X_2	Disastered Farmlands	1000 Ha
	X_3	Collapsed Houses	million rooms
	X_4	Number of Damaged Dams	one
	X_5	Length of Damaged Dams	km
	X_6	Direct Economic Losses	100 million RMB
Regional Economic Development Level	X_7 (-)	Per Capital GDP	yuan
	X_8 (-)	Per Capital Urban Disposable Income	yuan
	X_9 (-)	Local Financial Revenue	100 million yuan
	X_{10} (-)	Number of Sanitary Beds	Sets/10000 persons
	X_{11} (-)	Number of Graduates from Higher Education Instiution	one
	X_{12} (-)	Insurance Density	%
	X_{13} (-)	Insurance Penetration	%

(-) sign represents the negative relationship between the indicator and flooding risk vulnerability. The data is available in the Bulletin of Flood and Drought Disasters in China and the Provincial Yearbook 2019.

seven primary geographical divisions of China: Northeast, North, Northwest, Southwest, South, East and Central China, including Shanghai, Jiangxi, Zhejiang, Sichuan etc.

Besides the direct economic loss, another 12 indexes listed in Table 2 below are also selected as the evaluation criteria for flooding disasters, among which the vulnerability level of flooding disasters can be mainly divided into two parts: risk exposure and regional economic development level, which are from *the Bulletin of Flood and Drought Disasters in China* and *the Provincial Yearbook 2019*, respectively.

To summary, the economic loss caused by severe floods behaves with certain regional difference and highly correlated relationship with extreme precipitations. In the following section, we will establish extreme models to conduct the flooding risk management through the insurance, reinsurance and financial markets.

3. MAIN RESULTS

In risk management, of importance is to design a layered compensation among all stakeholders and diversify potential risk in insurance, reinsurance and financial markets. This section will give the main results concerning the extreme models of flooding economic losses and precipitations in Section 3.1, which will be applied to determine layered compensation scheme as well as the natural disaster risk in the price of flooding catastrophe bond in Section 3.2 and 3.3, respectively.

3.1. Extreme analysis of flooding economic losses and precipitations. In this section, we apply Extreme Value Theory (EVT) to analyse the tail distribution law of the economic loss caused

by severe floods. Given the limited datasets, we consider the compound Poisson Process of excess loss over a high threshold with severity following generalized Pareto distribution and Poisson frequency distribution. More specifically, let S_N be the total excess loss during 2006-2018, given by

$$S_N = \sum_{i=1}^N X_i,$$

where X_i 's are the excess loss before Year t and $N = N(t) \sim \text{Poisson}(\lambda t)$ is the number of severe floods or excess losses before Year t . Suppose that N and X_i 's are independent. Thus, the expected total loss is obtained by (cf. (5.4))

$$(3.1) \quad \mathbb{E}\{S_N\} = \mathbb{E}\{N\} \mathbb{E}\{X\} = \lambda \left(\frac{u}{1-\xi} + \frac{\sigma - \xi\mu}{1-\xi} \right),$$

where λ is the mean occurrence of extreme economic loss over certain threshold u specified below, and (μ, σ, ξ) is the triplet of parameter involved in the generalized extreme value distribution (GEV) in (5.2). In the following, we employ the mean residual life plot and variation plot to determine the economic loss threshold which helps to identify the GP distributed excess losses X_i 's.

We see from Figure 4 that the mean residual life plot tends to be linear in threshold within 15 to around 30. The stability of parameter estimates across the reduced threshold range 15 to 30 are demonstrated in the variation plots. Short bars are relatively better choices. Among them, a lower value of the threshold is suggested by [3] in order to ensure enough exceedances for accurate maximum likelihood estimate (MLE). As a result, threshold u is set as 17.19, the corresponding 70% empirical quantile.

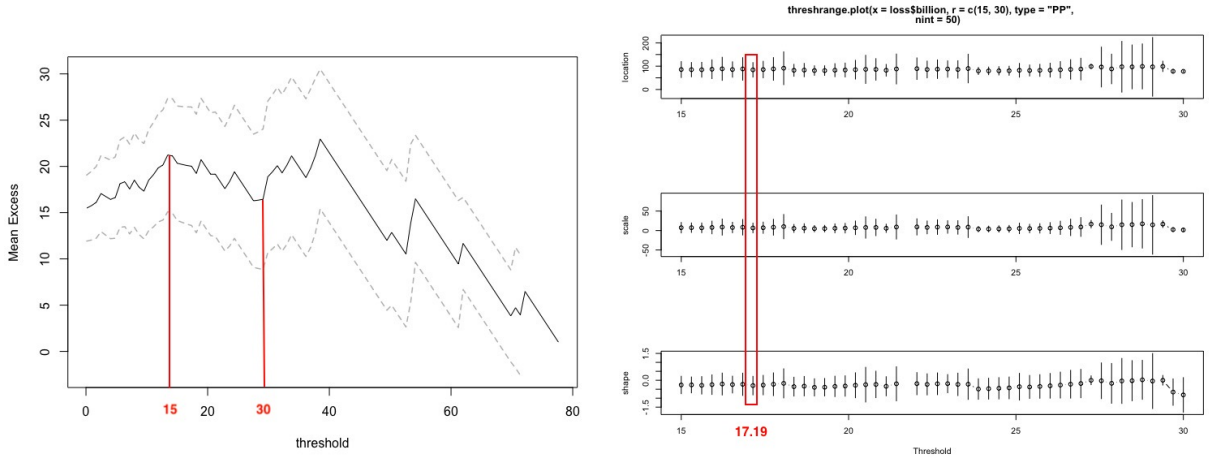


FIGURE 4. Mean residual life plot of economic loss (in billion yuan) with grey dash line representing 95% confidence interval (left). Variation plots of location, scale, and shape (from above to bottom) against threshold $u \in (15, 30)$ (right).

Now, we apply the excess models given in Section 5.1, namely we fit the excess losses by Point Process, compared with GP model and exponential model (the reduced model of GP with $\xi = 0$)

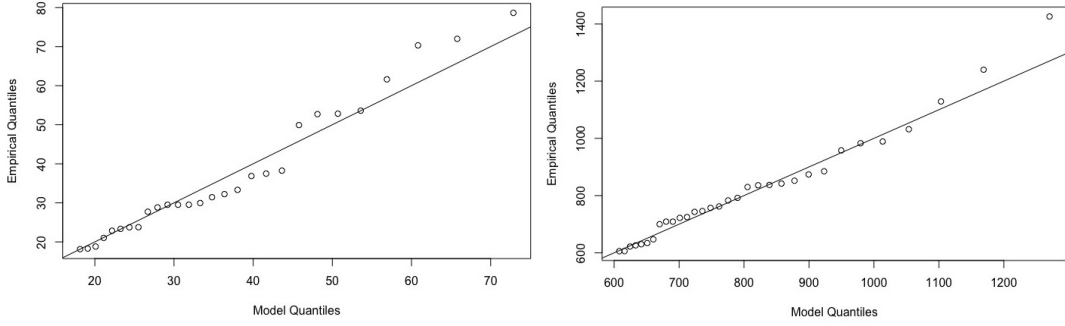


FIGURE 5. QQ plot of economic loss (left) and maximum point precipitation (right).

as well. The obtained estimates of the parameters are shown in Table 3. We see that Point Process model with minimum AIC and BIC is a challenging model to fit the excess losses. We get the maximum-likelihood estimate of the location, scale, and shape parameters of (μ, σ, ξ) is obtained by maximizing (5.6) as follows.

$$(\hat{\mu}, \hat{\sigma}, \hat{\xi}) = (83.34, 6.64, -0.29).$$

Similar procedure applies in the threshold excess of maximum point precipitation and gives the threshold of 626 and parameter estimated given in Table 8 in Section 3.3.

We also carry out the log-likelihood ratio test between PP model and GP (exponential) model. It turns out that PP model overwhelms the other two models with $p \leq 2.2 \times 10^{-16}$. Diagnostic plots of the PP model and GP model for threshold economic loss and precipitation are displayed in Figure 5. Points in these two figures can be generally considered as close to the unit diagonal, which means that exceedances are well fitted to the presupposed model.

TABLE 3. AIC, BIC and estimates of location, scale and shape parameters with standard errors in parentheses when fitting economic excess losses by Point Process, Generalized Pareto and Exponential models. Here threshold $u = 17.19$.

Model	Location parameter (μ)		Scale parameter (σ)		Shape parameter (ξ)		AIC	BIC
	Estimates (s.e.)	95% CI	Estimates (s.e.)	95% CI	Estimates (s.e.)	95% CI		
Point Process	83.34 (16.11)	(52.77, 115.91)	6.64 (6.44)	(-5.99, 19.27)	-0.29 (0.27)	(-0.81, 0.23)	22.16	26.16
Generalized Pareto	-	-	27.11 (7.96)	(11.50, 42.71)	-0.32 (0.23)	(-0.78, 0.13)	226.76	229.42
Exponential	-	-	20.18 (3.81)	(12.71, 27.66)	-	-	226.27	227.60

To get the expected total annual loss, it remains to check if the frequency of excess loss follows Poisson distribution. We employ Kolmogorov-Smirnov test and obtain p -value equal 0.3626, which suggests a good Poisson fit resulting in $\hat{\lambda} = 2.55$. Consequently, the total annual economic loss is estimated as RMB $2.55 \times 33.84 = 86.29$ billion.

Note that VaR and CVaR are two common risk measures applied to evaluate the extreme risks with good mathematical properties in insurance and finance fields. Applying extrapolation approach (c.f. (5.3) and (5.5)), Table 4 shows the estimates of VaR and CVaR values at different confidence levels

formalizing the compensation system. Its back-testing shows the efficiency of all estimates in Table 5. For both VaR and CVaR models, its spillover rate as a degree of risk coverage is fairly close to the significance value, implying the accurate estimate.

In particular, we specify four loss levels of compensation mechanism using the VaR and CVaR values, which can be covered among all stakeholders, including the insurers, local government, reinsurance and government fund like catastrophe bond. Besides the small parts of loss level (less than 85% VaR) covered by the insurers, we consider a zoning insurance fund for the moderate insurance cover (between 85% VaR and 90% CVaR) in Section 3.2. While for the higher loss level, the insurance companies may generally transfer the larger risk to reinsurance as well as the financial markets in terms of various financial securities ([14, 18]). Thus, in Section 3.3 we investigate the price of flooding catastrophe bond.

TABLE 4. Design of compensation mechanism.

Confidence level	VaR	CVaR	Loss level	Loss amount (billion)	Loss taker
97.5%	58.26	75.77	Fourth level	> 64.70	Government (CAT bond)
95.0%	46.97	64.70	Third level	53.48–64.70	Re-insurance
90.0%	35.53	53.48	Second level	28.76–53.48	CRFCIF*
85.0%	28.76	46.85	First level	< 28.76	Insurer

CRFCIF*: Cross-Regional Flooding Catastrophe Insurance Fund.

TABLE 5. Value and spillover rate of VaR and CVaR.

Significance value	VaR			CVaR		
	Value	Theoretical spillover (%)	Actual spillover (%)	Value	Theoretical spillover (%)	Actual spillover (%)
1.0%	72.94	1(1.0%)	1(1.06%)	90.16	1(1.0%)	0(0.00%)
2.5%	58.26	2(2.5%)	4(4.26%)	75.77	2(2.5%)	1(1.06%)
5.0%	46.97	5(5.0%)	8(8.51%)	64.70	5(5.0%)	3(3.19%)
10%	35.53	9(10%)	11(11.70%)	53.48	9(10%)	5(5.32%)
15%	28.76	14(15%)	19(20.21%)	46.85	14(15%)	8(8.51%)

3.2. Design of Cross Regional Compensation. This section is devoted to the design of zoning insurance level according to its flooding vulnerability. We apply two common approaches in terms of Multiple-Criteria Decision-Making in Appendix 5.2. Comparison analysis of the rank of the 19 flood-prone provinces is conducted according to the selection of risk indicators (cf. Table 2) and ranking indices given by Grey Relational Analysis (GRA) and the Technique for Order Preference by Similarity to an Ideal Solution (TOPSIS), see Appendices 5.2.1 and 5.2.2.

3.2.1. *Ranking of flooding vulnerability via Grey relational analysis (GRA)*. Grey relational analysis (GRA) is one of the most significant multivariate statistical analysis methods in the field of Grey System, which is mainly used to evaluate the relative performance or optimize multi-parameters to obtain the best quality characteristics among different discrete sequence ([8], [17], [11]). Given the original small sample size of the rare extreme flooding events involved, it seems that the GRA may be the best method to do this study since it is commonly used in dealing with problems of sample size and distribution uncertainty ([7]). Hence, we shall primarily implement the grey relational analysis method to evaluate and make a classification to the vulnerability level (premium level) for 19 provinces in China, based on the indicators relevant with flooding risks in 2019 (see Table 2 in Section 2 above). This will be helpful for future insurance premium allocation.

Based on the algorithm of grey relational grade calculation in Appendix 5.2.1, Table 6 shows the flooding risk ranking of 19 provinces and compares the rank if we select risk exposure indexes and exclude (include) the consideration of economic development level in different regions (see also Figure 6).

TABLE 6. Rank of each province in flooding vulnerability based on all indicators (left) and without regional economic indicators (right). Equal weight applies in the grey relational analysis.

Province	Grey Relational Grade A	Ranking	Province	Grey Relational Grade B	Ranking
Jiangxi	0.6882	1	Jiangxi	0.6299	1
Heilongjiang	0.6867	2	Heilongjiang	0.6234	2
Hunan	0.6468	3	Shandong	0.5994	3
Yunnan	0.6027	4	Hunan	0.5679	4
Gansu	0.5846	5	Zhejiang	0.4935	5
Shandong	0.5823	6	Sichuan	0.4780	6
Anhui	0.5792	7	Guangdong	0.3826	7
Sichuan	0.5687	8	Shanxi	0.3624	8
Shanxi	0.5605	9	Hubei	0.3611	9
Jilin	0.5535	10	Jilin	0.3591	10
Inner Mongolia	0.5431	11	Gansu	0.3494	11
Hubei	0.5154	12	Yunnan	0.3484	12
Chongqing	0.5149	13	Chongqing	0.3449	13
Zhejiang	0.5109	14	Anhui	0.3441	14
Henan	0.4953	15	Henan	0.3414	15
Shanghai	0.4390	16	Inner Mongolia	0.3396	16
Guangdong	0.4344	17	Jiangsu	0.3361	17
Beijing	0.4207	18	Beijing	0.3334	18
Jiangsu	0.4118	19	Shanghai	0.3334	19

We see that three zoning categories A, B and C with high, moderate and low premium payments can be determined according to the decreasing flood vulnerability of each province. Compared with the

results including regional economic development indicators, it is can be found that ranking location for many provinces has changed. This seems rational in view of [18] concerning the criterion of ‘either the area with serious loss or the developed area undertakes more’ in their study on Typhoon catastrophe. That means for some underdeveloped regions, the appropriate privilege can be undertaken for the insurance premium. For instance, Yunnan, Inner Mongolia and Gangsu drop while Shandong, Zhejiang and Jianguo rises to some extent. The change of ranking order can be largely interpreted by the economic development situation. In terms of descending order in some provinces, when collecting data, the economic development criterion of these provinces like per capita GDP, per capita disposable income and local fiscal revenue are found to be relatively lower than other provinces. Hence, it is significant to redistribute the initial capital of the flooding catastrophe fund to relieve the resource and financial burden in some less developed regions. And it is also obvious that the ascending ranking are often occurred in the coastal provinces like Shandong, Zhejiang, Shandong. This reflects these provinces may have more complete social security, more solid financial capacity, more cutting-edged medical facilities, and stronger risk prevention and protection awareness in supporting them to undertake possible flooding-related loss.

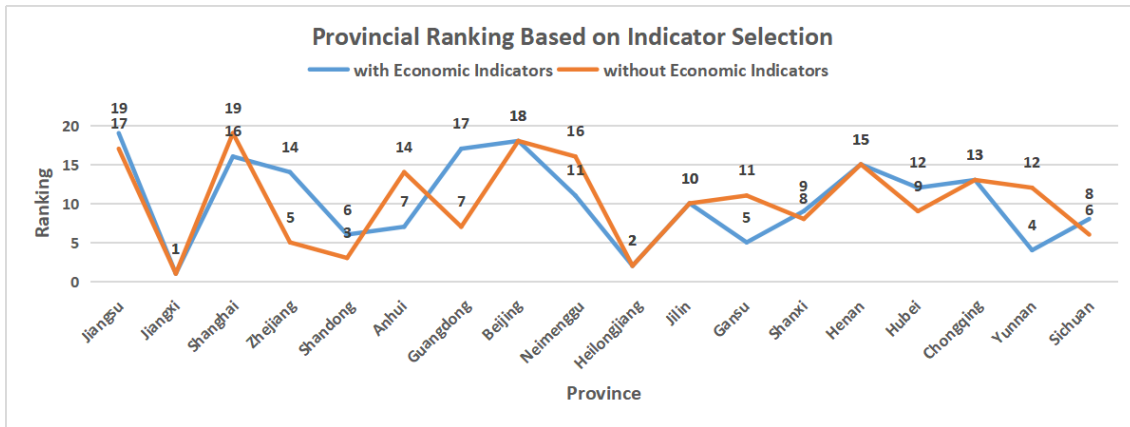


FIGURE 6. Provincial Ranking Based on Indicator Selection.

3.2.2. *The Technique of Order Preference by Similarity to an Ideal Solution (TOPSIS)*. In comparison of the result of grey relational analysis, this section is dedicated to the entropy weight method and The Technique for Order Preference by Similarity to an Ideal Solution (TOPSIS) based on closeness coefficient ([12]), see Section 5.2.2. Besides, the TOPSIS effectively reduces the influence from the subject choice of distinguishing coefficient involved in the GRA. Here, all 13 flooding risk indicators are included and the entropy weights apply in both GRA and TOPSIS.

Table 7 shows the rank of flooding vulnerability according to the calculated closeness coefficient and relational grade involved in TOPSIS and GRA. Note that the province with larger closeness coefficient implies the more severe flooding damage it may suffer from since it decreases in the relative distance to the highest risk vulnerability province compared to the lowest one, see Eq.

(5.11). We see most provinces (11 out of 19) get rather lower closeness coefficients, which are thus classified with low insurance premium level. On the other hand, most provinces remain steady ranking under GRA and TOPSIS except Anhui, Yunnan, Beijing and Guangdong (see Figure 7). There are several reasons accounting for this change. Different normalization method in GRA and TOPSIS method may explain this change. GRA method uses the linear normalization (also called min-max normalization), where the maximum and the minimum value of each feature of the dataset are used to scale the value of the feature to the interval $[0,1]$, achieving the equal scaling of the original data (Eq. (5.7)). While in TOPSIS, the minimum and maximum value are taken to divide an to be divided by original data respectively, to form a new sample dataset (Eq. (5.9)). Besides, from the entropy weight calculation results, higher weights are assigned to the original risk exposure indicators ($X_1 \sim X_6$), while weights of regional economic indicators are reduced to a lower level.

TABLE 7. Rank of each province in flooding vulnerability based on closeness coefficient (left) and GRA (right). The shannon entropy weights apply in both methods with all indicators taken into account.

Province	Closeness Coefficient	Ranking	Province	Grey Relational Grade	Ranking
Heilongjiang	0.5471	1	Heilongjiang	0.6422	1
Jiangxi	0.5180	2	Jiangxi	0.6124	2
Hunan	0.4879	3	Shandong	0.5782	3
Shandong	0.4819	4	Hunan	0.5711	4
Sichuan	0.3758	5	Sichuan	0.4902	5
Zhejiang	0.3288	6	Zhejiang	0.4729	6
Guangdong	0.1918	7	Shanxi	0.4371	7
Beijing	0.1914	8	Anhui	0.4308	8
Shanxi	0.1456	9	Yunnan	0.4269	9
Jilin	0.1282	10	Gansu	0.4200	10
Chongqing	0.1279	11	Jilin	0.4153	11
Gansu	0.1223	12	Inner Mongolia	0.4081	12
Inner Mongolia	0.1187	13	Chongqing	0.4040	13
Anhui	0.1156	14	Beijing	0.4005	14
Hubei	0.1151	15	Hubei	0.3977	15
Yunnan	0.1097	16	Guangdong	0.3970	16
Shanghai	0.0975	17	Henan	0.3801	17
Henan	0.0654	18	Shanghai	0.3787	18
Jiangsu	0.0300	19	Jiangsu	0.3572	19

3.3. Design of Flooding Catastrophic Bonds. Because of the low frequency and high severity features of flooding events, insurers and re-insurers are eager to hedge their risk. To this, the bond market is a sounding choice since investors looking for arbitrage opportunities and finally mitigate the loss of insurance products. Collateralize special purpose vehicles (SPVs) issue the CAT bond, which is usually issued and established by sponsors who are insurers and re-insurers. For the SPVs, the

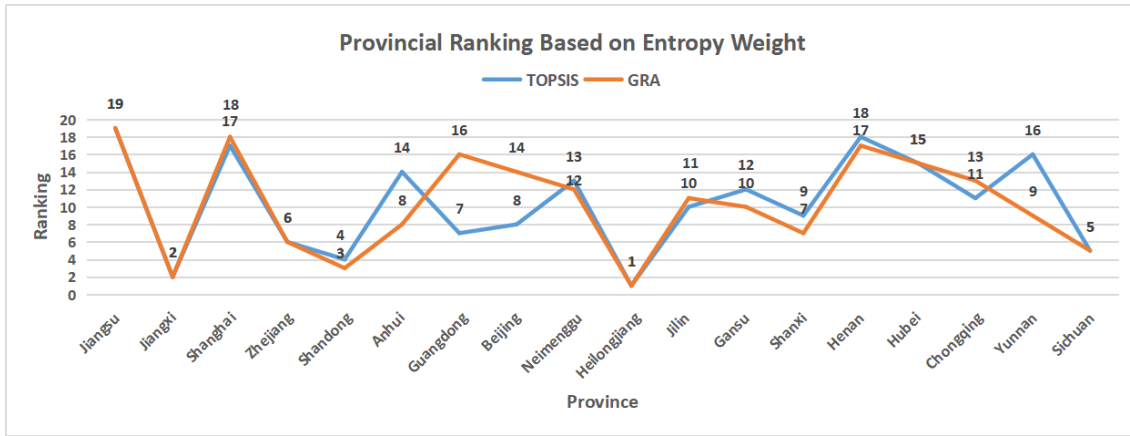


FIGURE 7. Provincial Ranking Based on Entropy Weight.

premium is received from the sponsors and reinsurance coverage are given in return. The rewarded premium usually is paid to the investor as a part of coupon payment and it contains a floating portion related to national reference rate. For example, London Interbank Offered Rate (LIBOR), Shanghai Inter-bank Offered Rate (Shior), can reflect the return from the trust account where the principal is deposited. The principal and coupon payments will be reduced whenever a specific triggering event happens. Also, some funds can be sent to the sponsor as a reimbursement for the claims. Here we follow the product pricing scheme proposed by [14] together with a compound Poisson trigger process similar to the 2015 Acorn Re earthquake CAT bond. The detailed workflow is presented in Figure 8

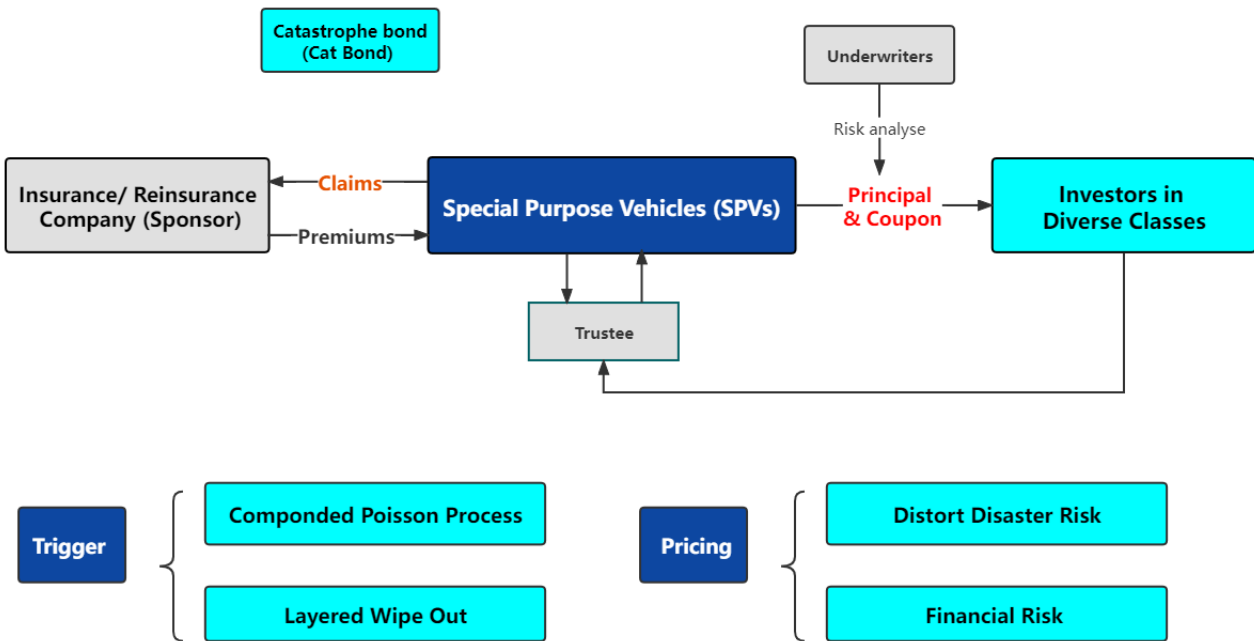


FIGURE 8. Operation mechanism for catastrophe bond.

Here, we consider a payoff function $\Pi(\cdot)$ and wipe out time τ defined by

$$\Pi(y) = \max\{1 - y, 0\}, \quad y \geq 0, \quad \tau = \inf\{t \geq 0 : \Pi(Y_t) = 0\}.$$

Here the trigger process $\{Y_t, t \geq 0\}$ is supposed as a compound Poisson trigger process given below

$$\begin{aligned} Y_t = & \sum_{j=1}^{N_t} (0.005 \times \mathbb{I}(X_j \in (626, 744]) + 0.015 \times \mathbb{I}(X_j \in (744, 849]) \\ & + 0.15 \times \mathbb{I}(X_j \in (849, 985]) + 0.2 \times \mathbb{I}(X_j \in (985, \infty))), \end{aligned}$$

where X_j denotes the severity of flooding driver (here max-point precipitation) and N_t denote the number of precipitation excess by time t . These four precipitation levels of 626, 744, 849 and 985 account for 0.7, 0.8, 0.9 and 0.95 quantile accordingly, which means when severity above certain level of threshold, a fraction 0.5%, 1.5%, 15%, 20% of principal will be wiped off.

Hence, for a $T = 3$ year CAT bond with face value $K = 1000$, in which each coupon period equals $\Delta = 1/4$, and hence coupons should be paid at times $s\Delta$, where $s = 1, \dots, 4T$. And it follows from Eq. (5.13), the price at time t becomes

$$\begin{aligned} (3.2) \quad P_0 = & \frac{K}{4} \mathbb{E}^{Q^1} \left[\sum_{s=1}^{\lfloor 4\tau \rfloor \wedge 4T} \mathbb{E}_t^{Q^2} [D(0, s\Delta) (R + i_{s\Delta}) \Pi(Y_{(s-1)\Delta})] \right] + KQ^1(\tau > T) \mathbb{E}^{Q^2} [D(0, T) \Pi(Y_T)]. \\ & + \frac{K}{4} \mathbb{E}^{Q^1} \left[(\tau - \lfloor 4\tau \rfloor \Delta) \mathbb{I}(\tau \leq T) \Pi(Y_{\lfloor \tau \rfloor}) \mathbb{E}^{Q^2} [D(0, \tau) (R + i_\tau) | \tau] \right]. \end{aligned}$$

Note that pricing scheme can only be realized by Monte-Carlo simulation. To this, we model the precipitation excess by generalized Pareto distribution $GP_{\xi, \beta}$. The threshold of $u = 600$ is determined by the mean residual plot and parameter variation plots, similar to that for excess economic loss in Figure 4. Meanwhile, we fit the annual occurrence process $\{N(t), t \geq 0\}$ of precipitation excess with Poisson distribution and get the intensity λ equals to 2.55. Furthermore, we implement a Wang's distortion of the disaster risk X ([16]), i.e.,

$$\tilde{X} = [(1 - \Phi(\Phi^{-1}(U) + \kappa))^{-\xi} - 1] \times \frac{\beta}{\xi} + u.$$

Additionally, the financial interest risk (r_t, ℓ_t) in Eq. (5.14) is fitted by the 4 year 3-month China treasury bond rates and 4 year 3-month Shanghai Inter-bank Offered Rate (Shibor). Estimated parameters are put into the pricing measure that combines a distorted pricing measure represent catastrophe insurance risk and risk-neutral pricing measure for the arbitrage financial market. The bond price is found by a simulation of 10^5 paths each with distorted generalized Pareto distributed inter-arrival time (severity of max-point precipitation excess).

Figure 9 shows the price varies in the financial market risk in term of the distortion parameter $\kappa \in (0, 1.5)$ of Wang's transform. A larger value of κ means a higher risk that investors are exposed to, so a higher premium they will require, and eventually a lower bond price. In addition, the practical value of $\kappa = 0.41$ is determined when it allows par value (1000) to be equal to the bond

TABLE 8. Specification of interest rate processes and precipitation distribution.

Panel A: Vasicek models (under Q^2)								
Risk-free rate				Shibor				Correlation
a_r	b_r	σ_r	r_0	a_ℓ	b_ℓ	σ_ℓ	ℓ_0	ρ
1.52	4.12%	1.40%	2.28%	0.04	2.02%	4.00%	2.43%	0.89
Panel B: Maximum point precipitation distribution								
Under \mathbb{P}^1				Under Q^1				
$\mathbb{P}\{X > u\} = 34\%$				$Q^1(X \leq x) = \Phi(\Phi^{-1}(P^1(X \leq x)) - \kappa)$				
$X - u (X > u) \sim GPD_{\gamma, \beta}$				$\kappa = 0.42$				
$\gamma = -0.181, \beta = 258.55$								
$u = 600$								
Maximum magnitude: 2032.31								

price. Furthermore, the sensitivity test is conducted for its shape parameter, presenting in Figure 9. At this time, the ratio of scale (β) to shape (ξ) remains to be -1432.311 , which means the maximum (the right endpoint) is kept unchanged as 2032.31. It turns out that, the bond price increases in negative shape parameter, which is reasonable in reality as investors are exposed to higher risk and require lower cost/ higher return at this time.

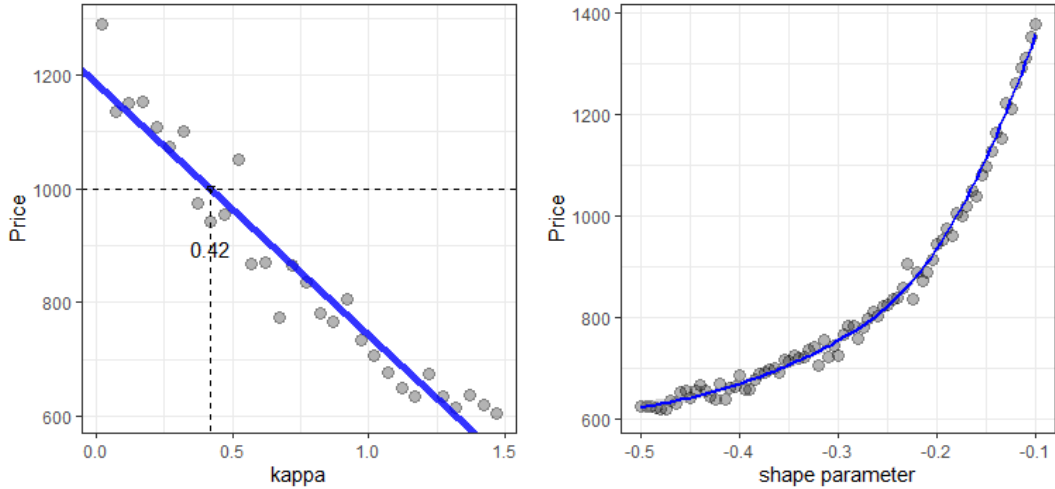


FIGURE 9. The price at $t = 0$ varies in the distortion parameter κ (left) and in the shape parameter ξ (right). Here, we simulate 10^5 samples of the threshold excess of point precipitation from $GPD_{\xi, \beta}$. The other parameters specified in Table 8 for the left plot, and we keep $\beta/\xi = -1432.311, \kappa = 0.42$ for the right plot.

4. CONCLUSIONS

This paper addresses the layered compensation scheme of flood-caused economic loss and the cross-regional insurance fund in the framework of extreme value theory and multiple-criteria decision-making. Besides, to mitigate the risk among insurers and reinsurers, further study on flood catastrophe bond price is conducted to reflect both the financial market risks and potential disaster risk with the primary flood driver of extreme precipitations as triggers. We provide the government and the local flooding disaster risk management with the catastrophic funding operation mechanism. Moreover, the risk management policymakers should consider regional difference among the disaster risk exposures, the economic development level and the local living conditions. The financial securities including natural disaster bonds can relieve the traditional insurance companies' pressure and disperse the possible huge loss into both insurance company and capital markets, which can return attract more investors to participate in the risk dispersion and transfer of flooding catastrophes.

5. APPENDIX

5.1. Extreme Value Theory. Extreme value theory is a natural tool to model severe floods and its caused economic losses since few extreme precipitations results in more than 90% annual economic losses. The flood risk management institutes should focus on the maxima and tail exposures instead of expected average outcome of compartmental models.

Given a high threshold u , suppose that the threshold excess of X is well fitted by a Generalized Pareto (GP) distribution $G(y; \sigma(u), \xi)$. Then the exceedance probability of X over larger x , can be represented as

$$(5.1) \quad 1 - F(x) = (1 - F(u))\mathbb{P}\{X > x | X > u\} \approx (1 - F(u)) \left(1 + \xi \frac{x - u}{\tilde{\sigma}}\right)^{-1/\xi}, \quad x > u.$$

With suitable threshold u , we get n_u excesses $(x_i - u)$'s leading to the maximum likelihood estimate of ξ and $\tilde{\sigma} = \tilde{\sigma}(u) = \sigma + \xi(u - \mu)$. Here (μ, σ, ξ) is the triple of location, scale and shape parameter involved in the GEV model fitting the block maxima M_n of an independent and identically distributed sample $X_1, \dots, X_n \sim X \sim F$, i.e.,

$$(5.2) \quad \mathbb{P}\{M_n \leq x\} \approx G(x; \mu, \sigma, \xi) := \exp\left(-\left(1 + \xi \frac{x - \mu}{\sigma}\right)_+^{-1/\xi}\right)$$

holds under regular conditions.

The exceedance probability in (5.1) provides information on the amount of time a risk is expected to exceed certain performance levels, which is commonly used to predict extreme events such as floods, hurricanes and earthquakes. In addition, one may invert (5.1) to obtain a high quantile of the underlying distribution or T -year return level stated below.

For $T > 1/\bar{F}(u)$, we have the T -year return level (i.e., the level x_T that is exceeded on average every T observations (with probability $p = 1/T$) is

$$x_T = u + \frac{\tilde{\sigma}}{\xi} \left(\left(\frac{1}{T\bar{F}(u)} \right)^{-\xi} - 1 \right).$$

Thus, the minimum level that the potential risk is exceeded with small probability $1 - q$, the so-called Value-at-Risk (VaR) at level q , denoted by $\text{VaR}_q(X)$, is given by

$$(5.3) \quad \text{VaR}_q(X) = u + \frac{\tilde{\sigma}}{\xi} \left(\left(\frac{1 - q}{\bar{F}(u)} \right)^{-\xi} - 1 \right), \quad q > F(u).$$

VaR is commonly used as a risk measure to determine the potential capital premium due to its simplicity and back-testing properties. However, it does not reflect the tail magnitude but its probability. Alternatively, conditional Value-at-Risk (CVaR) is the expected value of the losses exceeding the corresponding VaR, so it is represented as

$$\text{CVaR}_p(X) = \mathbb{E} \{X | X > \text{VaR}_p(X)\} = \text{VaR}_p(X) + \mathbb{E} \{X - \text{VaR}_p(X) | X > \text{VaR}_p(X)\}.$$

Since the threshold-excesses follow asymptotically generalized Pareto distribution, one may approximate the tail expectations as

$$(5.4) \quad \mathbb{E} \{X - u | X > u\} \approx \frac{\tilde{\sigma}(u)}{1 - \xi} = \frac{\sigma + \xi(u - \mu)}{1 - \xi}, \quad \xi < 1.$$

Thus,

$$(5.5) \quad \text{CVaR}_p(X) = \text{VaR}_p(X) + \frac{\tilde{\sigma}(\text{VaR}_p(X))}{1 - \xi} = \frac{\text{VaR}_p(X)}{1 - \xi} + \frac{\sigma - \xi\mu}{1 - \xi}.$$

One can obtain estimates of exceedance probability, VaR and CVaR using Eq. (5.1), (5.3) and (5.5) with related parameters estimated and empirical survival probability $\hat{F}(u) = n_u/n$ provided that n_u exceedances over u come from n samples.

Besides the GEV and GP models the block maxima and threshold excesses aforementioned, a particularly elegant formulation of characterizing the extreme value behavior is derived from the theory of point processes (PP) which consider exceedances of threshold as events in time and model thus both the occurrence and intensity of exceedances. Given a sequence of r.v. X_i 's with values in a state space \mathcal{A} , we define, for any set $A \subset \mathcal{A}$, the r.v. $N(A)$ is the number of points X_i in the set A , which can formulize a point process under certain conditions. The intensity measure of this process is one of the key summary features, defined as

$$\Lambda(A) = \mathbb{E} \{N(A)\},$$

which gives the expected number points in any subset A . The intensity density function is then defined by its derivative function if this exists with $A = \prod_{i=1}^d [a_i, x_i]$, i.e.,

$$\lambda(x) = \frac{\partial \Lambda(A)}{\partial x_1 \cdots \partial x_d}.$$

Let X_1, \dots, X_n be an independent and identically distributed sequence, which may consists of the observation of a potential risk X satisfying (5.1) or (5.2). Then the point process of $(i/(n+1), X_i)$ on $A = [t_1, t_2] \times (u, \infty) \subset [0, 1] \times \mathbb{R}$, denoted by $N(A)$, is given as

$$N(A) := \#\{i \in \mathbb{N}, t_1 \leq i/(n+1) \leq t_2, X_i > u\}, \quad A = [t_1, t_2] \times (u, \infty).$$

Under some weak conditions, we have $N(A) \sim \text{Poisson}(\Lambda(A))$ holds asymptotically with intensity measure given as below.

$$\Lambda(A) = \int_{(t,x) \in A} \lambda(t, x) dt dx = (t_2 - t_1) \cdot \left[1 + \xi \frac{u - \mu}{\sigma} \right]^{-\frac{1}{\xi}} \cdot \mathbb{I}(1 + \xi \cdot (u - \mu)/\sigma > 0),$$

where $\mu, \xi \in \mathbb{R}$, and $\sigma > 0$, which are the so-called location, shape, and scale parameter, respectively. $\mathbb{I}(\cdot)$ is the indicator function, see Theorem 7.1.1 [3]. Maximum likelihood estimation is adopted here to estimate parameters involved in the PP model. PP log-likelihood, $\ell(\cdot)$, for a high threshold u , is given as

$$(5.6) \quad \ell(\mu, \sigma, \xi; x_1, \dots, x_n) \\ = -n_u \ln \sigma - \left(\frac{1}{\xi} + 1 \right) \sum_{i=1}^n \ln \left(1 + \frac{\xi}{\sigma} (x_i - \mu) \right) \mathbb{I}(x_i > u) - \left(1 + \frac{\xi}{\sigma} (u - \mu) \right)^{-\frac{1}{\xi}}.$$

Though this log likelihood function considers excesses, the parametrization is based on the GEV distribution function, and thus is invariant to threshold. Consequently, the PP model can be adapted to allow for non-stationary effects to include temporal or covariate effects in the parameters with even time-varying thresholds ([6]).

5.2. Multiple-Criterion Decision-Making Method (MCDM). Multiple-Criterion Decision-Making Method (MCDM) provides support for decision-makers to make the optimal choice among various alternatives and criteria. Here we consider two most useful methods of MCDM, namely, GRA and TOPSIS:

- (1) Grey relational analys (GRA) is commonly used to tackle the problem of sample size and data uncertainty and achieve ranking objects by the relation degree to the reference object based on its performance matrix and distinguishing coefficient.
- (2) The Technique for Order Preference by Similarity to an Ideal Solution (TOPSIS) can reduce the influence from the subject choice of distinguishing coefficient involved in GRA. In the application of TOPSIS, we consider Shannon entropy weights to determine the decision matrix and model the relative distance of the Positive-ideal solution to the Negative-ideal solution.

Both methods require the data normalization due to the different measurement of units and magnitude. In Section 5.2.1 and 5.2.2, we will illustrate how to give grey relational grade and closeness coefficient which will be used to rank the alternatives, see (5.8) and (5.11) below.

5.2.1. *Grey relational analysis (GRA)*. Once we have the performance information of n alternatives on p criteria, say $(x_{ij})_{n \times p}$, we shall select and combine the most representative data of each indicator as the reference sequence x_0 . Grey relational coefficients are calculated between the reference sequence and all other comparability sequences. According to the calculated grey relational coefficients, grey relational grade can be achieved. Finally, if we sort the grade into a table, in this paper, the result with the highest grey relational coefficient will be the province most affected by the flooding damages. The specific description of steps are as follows.

Step 1: Dimensionless processing (Normalization). Suppose $X_j = (x_{1j}, x_{2j}, \dots, x_{nj})^\top$, $j = 1, \dots, p$ is the performance of n alternatives on the j th criterion. To unify the indicators, normalization should be applied. We consider the normalization of "the larger the better" and "the smaller the better" criteria to standardize the data as follows.

$$(5.7) \quad x'_{ij} = \begin{cases} \frac{x_{ij} - \min_i(x_{ij})}{\max_i(x_{ij}) - \min_i(x_{ij})}, & \text{for positive-correlated indicators,} \\ \frac{\max_i(x_{ij}) - x_{ij}}{\max_i(x_{ij}) - \min_i(x_{ij})}, & \text{otherwise.} \end{cases}$$

Since the flooding risk vulnerability has positive correlation with disaster losses, that is, the higher the risk vulnerability, the greater the loss the province will face. Based on two parts in this paper, risk exposure indexes are positively correlated with the flooding risk vulnerability (the larger the risk exposure indicators, the higher risk vulnerability); however, the regional economic development level indexes show negatively correlation with the flooding risk vulnerability. Hence, the regional economic development level indexes are still needed to be inverted, normalizing the data according to "the smaller the better".

Step 2: calculate Grey relational coefficients. Since the normalized data x'_{ij} 's represent the scale of flooding risks, the largest data of each indicator can be taken as the most vulnerability representative, which are selected as a reference sequence $x_0 : x_0 = (x_{01}, x_{02}, \dots, x_{0p})^\top = \mathbf{1}$ in view of Eq. (5.7). In the following, we calculate the grey relational coefficient to measure the similarity of the i th alternative (province) performed on the j th indicator.

$$\tau(x_{0j}, x_{ij}) = \frac{\min_{ij} |x_{0j} - x_{ij}| + \xi \max_{ij} |x_{0j} - x_{ij}|}{|x_{0j} - x_{ij}| + \xi \max_{ij} |x_{0j} - x_{ij}|} = \frac{\zeta}{|x_{0j} - x_{ij}| + \zeta}.$$

Here ζ represents distinguishing coefficient ranging from 0 to 1; the smaller ζ indicates larger distinguishing power; 0.5 is taken by default as many other papers.

Step 3: calculate grey relational grade. Grey relational grade is the weighed sum of grey relational coefficients obtained in Step 2, which shows the level of similarity between reference sample x_0 and all other comparable objects x_i . Equal weight is considered by default. The formula of grey relational grade is as follows.

$$(5.8) \quad \tau(x_0, x_i) = \sum_{j=1}^p w_j \tau(x_{0j}, x_{ij}), \quad \text{where } w_1 = \dots = w_p = 1/p, \quad p = 13.$$

The grade is in the range 0 to 1, the closer the grade to 1, the higher the vulnerability of the i th province.

GRA will rank the alternatives according to the grey relational grade given in Eq. (5.8). The larger the grade is, the higher vulnerability the alternative has. In the following, we consider an alternative approach to measure the vulnerability, namely, the TOPSIS.

5.2.2. *Technique for Order Preference by Similarity to an Ideal Solution (TOPSIS)*. In contrast with GRA, TOPSIS is free of distinguishing coefficient with a reasonable entropy distribution of weight for each criterion. Essentially, the ranking follows the relative distance to the extreme ideal solutions. This can be carried out following the steps below.

Step 1: calculate entropy and entropy weight. Based on the normalized data $x'_{ij} \in [0, 1]$ using Eq. (5.7), we amplify it with a small extent $a = 0.01$ and proceed the coordinate translation as

$$(5.9) \quad x''_{ij} = x'_{ij} + a, \quad r_{ij} = \frac{x''_{ij}}{\sum_{i=1}^n x''_{ij}}, \quad i = 1, 2, \dots, n; \quad j = 1, \dots, p.$$

Here, the amplitude a added to the dimensionless data is to eliminate the effect of the logarithmic calculation. The selection of $a = 0.05$ is motivated by [12] since then the resulted evaluation shows great significance.

Now, calculate the entropy for each criterion as

$$e_j = -\lambda \sum_{i=1}^n r_{ij} \ln r_{ij} \in [0, 1], \quad j = 1, 2, \dots, p,$$

where $\lambda = \frac{1}{\ln n}$, the Boltzman's constant. Finally, we obtain the entropy weight w_j of the j th indicator as

$$(5.10) \quad w_j = \frac{\bar{e}_j}{\sum_{j=1}^p \bar{e}_j}, \quad j = 1, 2, \dots, p,$$

where $\bar{e}_j = 1 - e_j$ models the degree of diversification e_j 's of the information.

Based on the calculated weight for each indicator, TOPSIS is applied to help determine the ideal scheme, that is the province with the highest and lowest flooding risk vulnerability in this paper.

Step 2: construct weighted normalized decision matrix V .

$$R = \begin{pmatrix} r_{11} & \cdots & r_{1p} \\ \vdots & \ddots & \vdots \\ r_{n1} & \cdots & r_{np} \end{pmatrix}, \quad r_{ij} = \begin{cases} \frac{x_{ij}}{\max_i(x_{ij})}, & \text{positive-correlated indicators,} \\ \frac{\min_i(x_{ij})}{x_{ij}}, & \text{otherwise.} \end{cases}$$

Thus, we obtain the weighted normalized decision matrix V .

$$V = (v_{ij})_{np}, \quad \text{with } v_{ij} = w_j r_{ij},$$

where the weights w_j 's are given by entropy method in Eq. (5.10).

Step 3: calculate the positive-ideal solution (PIS) and the negative-ideal solution (NIS).

$$\begin{cases} A^+ = \{v_1^+, v_2^+, \dots, v_p^+\}, & v_j^+ = \max_i (v_{ij}), \\ A^- = \{v_1^-, v_2^-, \dots, v_p^-\}, & v_j^- = \min_i (v_{ij}). \end{cases}$$

Step 4: calculate the distance of each object from PIS and NIS.

$$S_i^+ = \sqrt{\sum_{j=1}^p (v_{ij} - v_j^+)^2}, \quad S_i^- = \sqrt{\sum_{j=1}^p (v_{ij} - v_j^-)^2}.$$

Step 5: calculate the closeness coefficient of each object.

$$(5.11) \quad C_i^* = \frac{S_i^-}{S_i^+ + S_i^-}, \quad 0 < C_i^* < 1.$$

5.3. A Pricing Scheme of Catastrophe Bond. Trigger model, payoff function, principal wipe out function and accrued coupon should be determined prior to pricing measurement since coupon payment and principal redemption might be changed once catastrophe (CAT) event occurs.

Consider a trigger process $\{Y_t, t \geq 0\}$ as a component-wise non-decreasing, non-negative, and right continuous stochastic process

$$(5.12) \quad Y_t = f(X_1, X_2, \dots, X_{N_t}), \quad t \geq 0,$$

where $\{X_n, n \in \mathbb{N}\}$ is a sequence of random variables modelling precipitation severity and $\{N_t, t \geq 0\}$ is a counting process to model the occurrence of floods, and f is a component-wise non-decreasing function.

There are various kinds of trigger Y , for instance

- (i) The aggregate amount of loss due to the flood;
- (ii) The number of earthquakes which consider both magnitude and frequency as below

$$Y_t = \sum_{j=1}^{N_t} \mathbb{I}(X_j > u), \quad u \geq 0,$$

where u is a high threshold and $N(t)$ is the number of the exceedances over the threshold observed in $[0, t]$.

Next, the pay off function $\Pi(y) : [0, \infty) \mapsto [0, 1]$, is a non-increasing function linking the natural disaster risks via the trigger process $Y_t = f(X_1, \dots, X_{N(t)})$ and the financial securities, stimulate a plan of allocating the principal between the investor and sponsor according to the development of triggering process. Specially, the time of principal wiped out is denoted by

$$\tau = \inf \{t \geq 0 : \Pi(Y_t) = 0\}.$$

Next, we introduce the pricing measure as a product of the natural disaster risk and financial risk. The pricing at time t is essentially the discounted value of future coupon payments plus the discounted

value of the remaining principal.

$$\begin{aligned}
(5.13) \quad P_t &= K \mathbb{E}_t^{Q_1 \times Q_2} \left[\sum_{s=\lfloor t \rfloor + 1}^{\lfloor \tau \rfloor \wedge T} D(t, s)(R + i_s) \Pi(Y_{s-1}) + D(t, \tau) \mathbb{1}(\tau \leq T) + D(t, T) \Pi(Y_{s-1}) \right] \\
&= K \mathbb{E}_t^{Q_1} \left\{ \sum_{s=\lfloor t \rfloor + 1}^{\lfloor \tau \rfloor \wedge T} \Pi(Y_{s-1}) \mathbb{E}_t^{Q_2} [D(t, s)(R + i_s)] \right\} + K \mathbb{E}_t^{Q_1} [\Pi(Y_T)] \mathbb{E}_t^{Q_2} [D(t, T)], \\
&\quad + K \mathbb{E}_t^{Q_1} \left\{ (\tau - \lfloor \tau \rfloor) \Pi(Y_{\lfloor \tau \rfloor}) \mathbb{I}((\tau \leq T)) \mathbb{E}_t^{Q_2} [D(t, s)(R + i_s) | \tau] \right\},
\end{aligned}$$

where the pricing measure Q_1 is the distorted probability measure of the catastrophe disaster risk X , $\mathbb{E}_t^{Q_1}[\cdot]$ terms usually require simulation to evaluate.

The performance of financial market is reflected by the interest rate process $r_t, t \geq 0$ and the Shi-bor process $\ell_t, t \in N$ using a risk-neutral pricing measure Q_2 for the arbitrage-free financial market according to the well-established APT to price the interest rate risk. We link the financial market risks with Eq. (5.13) through

$$D(t, T) = \exp \left(- \int_t^T r_t dt \right), \quad i_t = e^{\ell_t} - 1.$$

We model $\{(r_t, \ell_t), t \geq 0\}$ as a bivariate correlated Ornstein-Uhlenbeck (OU) process (i.e., Vasicek models [10]) under the risk-neutral measure Q_2 , denoted by

$$(5.14) \quad \begin{cases} dr_t = a_r(b_r - r_t) dt + \sigma_r dW_{r,t}, \\ d\ell_t = a_\ell(b_\ell - \ell_t) dt + \sigma_\ell dW_{\ell,t}, \end{cases}$$

where a, b and σ are positive numbers corresponding to the rate of mean reversion, the long run mean, and the volatility, accordingly. And $W_{r,t}$ is a standard Brownian Motion under Q_2 . Here the two Brownian motion processes are constant correlated, i.e., for some for some $\rho \in (-1, 1)$,

$$dW_{\ell,t} dW_{r,t} = \rho dt, \quad t \geq 0.$$

It follows from the appendix of [14], we have (see also [10])

$$(5.15) \quad \mathbb{E}_t^{Q_2} [D(t, s)] = A(t, s) e^{-B(t, s)r_t}, \quad s \geq t \geq 0,$$

where

$$\begin{cases} A(t, s) = \exp \left\{ \frac{(B(t, s) - (s - t)) (a_r^2 b_r - \sigma_r^2 / 2)}{a_r^2} - \frac{\sigma_r^2 B(t, s)^2}{4a_r} \right\}, \\ B(t, s) = \frac{1 - e^{-a_r(s-t)}}{a_r}. \end{cases}$$

And $\mathbb{E}_t^{Q_2} [D(t, s)i_s]$ can be calculated by

$$\begin{aligned}
(5.16) \quad \mathbb{E}_t^{Q_2} [D(t, s)i_s] &= \mathbb{E}_t^{Q_2} [D(t, s)e^{\ell_s}] - \mathbb{E}_t^{Q_2} [D(t, s)] \\
&= \tilde{A}(t, s) \exp \left\{ -B(t, s)r_t + \tilde{B}(t, s)\ell_t \right\} - A(t, s) e^{-B(t, s)r_t}, \quad s \geq t \geq 0,
\end{aligned}$$

where $A(\cdot, \cdot)$ and $B(\cdot, \cdot)$ are defined as above, and $\tilde{A}(\cdot, \cdot)$ and $\tilde{B}(\cdot, \cdot)$ are introduced as below.

$$\begin{cases} \tilde{A}(t, s) = \exp \{ - (C_1(t, s) + C_2(t, s)) \}, \\ \tilde{B}(t, s) = e^{-a_\ell(s-t)} \end{cases}$$

with

$$\begin{cases} C_1(t, s) = \left(b_r - \frac{\sigma_r^2}{2a_r} \right) (s-t) + \frac{3\sigma_r^2}{4a_r^2} + \frac{\rho\sigma_r\sigma_\ell}{a_\ell(a_\ell - a_r)} + \frac{\sigma_\ell^2}{4a_\ell} + b_\ell - \frac{b_r}{a_r}, \\ C_2(t, s) = \frac{\sigma_r^2}{4a_r^2} e^{-2a_r(s-t)} + \left(\frac{b_r}{a_r} - \frac{\sigma_r^2}{a_r^2} \right) e^{-a_r(s-t)} + \left(\frac{\rho\sigma_r\sigma_\ell}{a_r a_\ell} - b_\ell \right) e^{a_\ell(s-t)} \\ \quad - \frac{\rho\sigma_r\sigma_\ell}{a_r(a_\ell - a_r)} e^{(a_\ell - a_r)(s-t)} - \frac{\sigma_\ell^2}{4a_\ell} e^{2a_\ell(s-t)}. \end{cases}$$

REFERENCES

- [1] Junfei Chen, Guiyun Liu, Liu Yang, Quanxi Shao, and Huimin Wang. Pricing and simulation for extreme flood catastrophe bonds. *Water Resources Management*, 27, 08 2013.
- [2] Pasquale Cirillo and Nassim Nicholas Taleb. Tail Risk of Contagious Diseases. *Nature Physics*, 16(6):606–613, 2020.
- [3] Stuart Coles. *An Introduction to Statistical Modeling of Extreme Values*. Springer Series in Statistics. Springer-Verlag, London, 2001.
- [4] Paul Embrechts, Claudia Klüppelberg, and Thomas Mikosch. *Modelling Extremal Events: for Insurance and Finance*, volume 33. Springer Science & Business Media, 2013.
- [5] Michael Falk, Jürg Hüsler, and Rolf-Dieter Reiss. Extreme Value theory. In *Laws of Small Numbers: Extremes and Rare Events*, pages 25–101. Springer, 2011.
- [6] Eric Gilleland and Richard W. Katz. extremes 2.0: An extreme value analysis package in R. *Journal of Statistical Software*, 72(8):1–39, 2016.
- [7] Chien-Ta Ho. Measuring Bank Operations Performance: an Approach Based on Grey Relation Analysis. *Journal of the Operational Research Society*, 57(4):337–349, 2006.
- [8] Deng Ju-Long. Control Problems of Grey Systems. *Systems & Control Letters*, 1(5):288–294, 1982.
- [9] Z.W. Kundzewicz, Jinlong Huang, I. Pinskiwar, Buda Su, M. Szwed, and Tong Jiang. Climate Variability and Floods in China - A Review. *Earth-Science Reviews*, 211:103434, 2020.
- [10] Rogemar S. Mamon. Three Ways to Solve for Bond Prices in the Vasicek Model. *Journal of Applied Mathematics and Decision Sciences*, 8(1):1–14, 2004.
- [11] Xinxin Peng, Xiaolei Tang, Yijun Chen, and Jinghua Zhang. Ranking the Healthcare Resource Factors for Public Satisfaction with Health System in China—Based on the Grey Relational Analysis Models. *International Journal of Environmental Research and Public Health*, 18(3):995, 2021.

- [12] Ruiling Sun, Zaiwu Gong, Ge Gao, and Ashfaq Ahmad Shah. Comparative Analysis of multi-criteria decision-making Methods for Flood Disaster Risk in the Yangtze River Delta. *International Journal of Disaster Risk Reduction*, 51:101768, 2020.
- [13] Swenja Surminski and Delioma Oramas-Dorta. Flood Insurance Schemes and Climate Adaptation in Developing Countries. *International Journal of Disaster Risk Reduction*, 7:154–164, 2014.
- [14] Qihe Tang and Zhongyi Yuan. CAT Bond Pricing: A Product Probability Measure with POT Risk Characterization. *ASTIN Bulletin*, 49(2):457–490, 2019.
- [15] Erin Towler, Dagmar Llewellyn, Andreas Prein, and Eric Gilleland. Extreme-Value Analysis for the Characterization of Extremes in Water Resources: A Generalized Workflow and Case Study on New Mexico Monsoon Precipitation. *Weather and Climate Extremes*, 29:100260, 2020.
- [16] Shaun S Wang. A Class of Distortion Operators for Pricing Financial and Insurance Risks. *Journal of Risk and Insurance*, pages 15–36, 2000.
- [17] Yue Zhao, Zaiwu Gong, Wenhao Wang, and Kai Luo. The comprehensive Risk Evaluation on Rainstorm and Flood Disaster Losses in China Mainland from 2004 to 2009: Based on the Triangular Gray Correlation the ory. *Natural Hazards*, 71, 03 2013.
- [18] Yan Zhou and Hai-ping Tu. Design of Cross-regional Typhoon Catastrophe Insurance Fund. *China Soft Science*, (6):69–80, 2017.

ACADEMY OF PHARMACY, XI'AN JIAOTONG-LIVERPOOL UNIVERSITY, SUZHOU, SIP 215123

Email address: Chengxiu.Ling@xjtlu.edu.cn

DEPARTMENT OF FINANCIAL AND ACTUARIAL MATHEMATICS, XI'AN JIAOTONG-LIVERPOOL UNIVERSITY, SUZHOU, SIP 215123

Email address: Jiayi.Li1802@student.xjtlu.edu.cn

DEPARTMENT OF FINANCIAL AND ACTUARIAL MATHEMATICS, XI'AN JIAOTONG-LIVERPOOL UNIVERSITY, SUZHOU, SIP 215123

Email address: Yixuan.Liu18@student.xjtlu.edu.cn

DEPARTMENT OF BIOLOGY INFORMATION, XI'AN JIAOTONG-LIVERPOOL UNIVERSITY, SUZHOU, SIP 215123

Email address: Zhiyan.Cai18@student.xjtlu.edu.cn